Available online at www.sciencedirect.com

ScienceDirect

European Journal of Mechanics A/Solids 27 (2008) 429–442

# A magnetoelectric screw dislocation interacting with a circular layered inclusion

Ming-Ho Shen *

*Department of Automation Engineering, Nan Kai Institute of Technology, 568 Chung Cheng Road, Tsao Tun, 542, Nantou County, Taiwan*

Received 23 June 2007; accepted 28 August 2007

Available online 31 August 2007

**Abstract**

Within the framework of the linear theory of magnetoelectroelasticity, the problem of a circular layered inclusion interacting with a generalized screw dislocation under remote anti-plane shear stress and in-plane magnetoelectric loads is investigated in this paper. The generalized dislocation can be located either in the matrix or in the circular layered inclusion. The layers are coaxial cylinders of annular cross-sections with arbitrary radii and different material properties. Using complex variable theory and the alternating technique, the solution of the present problem is expressed in terms of the solution of the corresponding homogeneous medium problem subjected to the same loading. Some numerical results are provided to investigate the influence of material combinations on the shear stress, electric field, magnetic and image force. These solutions can be used as Green's functions for the analysis of the corresponding magnetoelectric crack problem.


*Keywords:* Circular layered composite; Screw dislocation; Magnetoelectromechanical loadings

## 1. Introduction

Due to magnetoelectroelastic coupling behavior, piezoelectric/piezomagnetic composite materials are extensively used to design actuators, sensors and other electronic products in modern technology. Combining two or more distinct constituents, composite materials can take advantage of each constituent and consequently exhibit a superior magnetoelectroelastic effect. Van Suchtelen (1972) first reported that piezoelectric/piezomagnetic composites may exhibit a new property viz. the magnetoelectroelastic coupling effect. Later, van Run et al. (1974) observed that the magnetoelectric coefficients of a $BaTiO_3-CoFe_2O_4$ composite are two orders higher than the highest known magnetoelectric coefficients of a $Cr_2O_3$ medium. Studies of the properties of piezoelectric/piezomagnetic composites have been carried out by numerous investigators in recent years. Nan (1994) and Huang and Kuo (1997) proposed micromechanics models to estimate the effective properties of fibrous piezoelectric/piezomagnetic composite materials. Li (2000) and Wu and Huang (2000) studied the inclusion and inhomogeneity problems and predicted the magnetoelectric coupling coefficients of the piezoelectric/piezomagnetic composites. Pan (2001) and Chen et al. (2002) proposed micromechanics models to evaluate the effective properties of plane, layered piezoelectric/piezomagnetic composite

* Tel.: +886 49 2563489 x 3412; fax: +886 49 2565674.
*E-mail address:* mhshen@nkc.edu.tw.

0997-7538/$ – see front matter 
doi:10.1016/j.euromechsol.2007.08.004

materials. Wang and Shen (2003) obtained analytical solutions for the problem of inclusions of arbitrary shape in magnetoelectroelastic composites.

Dislocation solutions or Green's functions can serve as kernel functions for use in the singular integral equation method. They are one of the well-established tools in the solution of numerous problems in the mechanics and physics of solids. For example, Li and Dunn (1998a; 1998b) used three-dimensional magnetoelectroelastic Green's functions to study inclusion problems. Green's functions for magnetoelectroelastic solids have been studied by several authors. Liu et al. (2001) gave Green's functions for an infinite two-dimensional anisotropic magnetoelectroelastic medium containing an elliptical cavity or a crack. Li (2002) obtained explicit expressions for the magnetoelectric Green's functions for a transversely isotropic medium and used them to analyze the magnetoelectric inclusion and inhomogeneity problems. Recently, Fang et al. (2005) discussed the interaction between a generalized screw dislocation with circular-arc interfacial rigid lines in magnetoelectroelastic solids. Hao and Liu (2006) investigated the interaction between a screw dislocation and a semi-infinite crack in a transversely isotropic magnetoelectroelastic bimaterial. Zheng et al. (2007) discussed the interaction between a generalized screw dislocation with circular-arc interfacial cracks along a circular inhomogeneity in magnetoelectroelastic solids.

Because of the presence of materials such as fiber coatings or transitional layers between the inclusion and the matrix, it is more reasonable to regard an interface as an interphase layer with finite thickness. The three-phase models provide accurate predictions of the effective moduli of composite materials, and can be used to study the influence of the interphase layer on the shear stress, electric field and magnetic. The importance of three-phase models in composite mechanics research has been described by Xiao and Chen (2000), Jiang and Cheung (2001), Sudak (2003) and Liu et al. (2003). In this paper, we study the magnetoelectroelastic interaction between a generalized screw dislocation and a circular layered inclusion. The proposed method is based upon the technique of analytic continuation. It is alternately applied across the two concentric interfaces in order to derive the trimaterial solution in a series form, from the corresponding homogeneous medium solution. Following the introduction, a complex representation of anti-plane magnetoelectroelasticity is provided in Section 2 and solutions to the corresponding homogeneous medium, circular inclusion and circular layered inclusion problems are provided in Sections 3, 4 and 5, respectively. Several numerical examples are given and discussed in detail in Section 6.

## 2. A complex representation of anti-plane magnetoelectroelasticity

Consider a magnetoelectroelastic composite composed of three dissimilar materials bonded along two concentric circular interfaces. Each component is assumed to have the same material orientation with $x_3$ being the poling direction (Fig. 1). In a class of magnetoelectroelastic materials capable of undergoing out-of-plane displacement $w$, the in-plane electric potential is $\varphi$ and the in-plane magnetic potential is $\phi$, the governing field equations can be simplified to

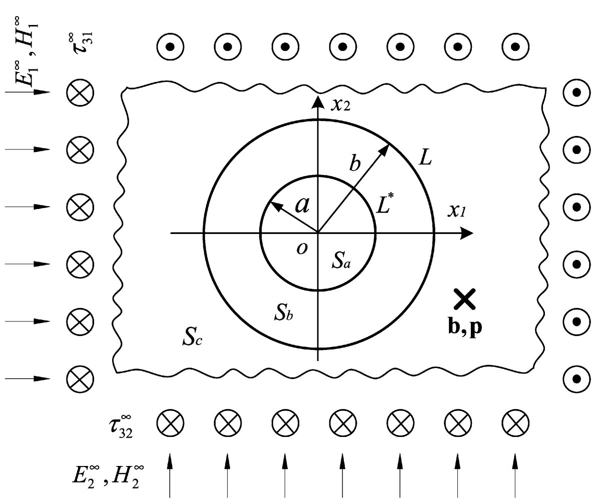


Fig. 1. A circular layered composite under magnetoelectromechanical loading.

$$c_{44}\nabla^2 w + e_{15}\nabla^2\varphi + q_{15}\nabla^2\phi = 0, \tag{1}$$

$$e_{15}\nabla^2 w - \varepsilon_{11}\nabla^2\varphi + d_{11}\nabla^2\phi = 0, \tag{2}$$

$$q_{15}\nabla^2 w - d_{11}\nabla^2\varphi + \mu_{11}\nabla^2\phi = 0, \tag{3}$$

where $\nabla^2$ is the two-dimensional Laplace operator, $c_{44}$ is a elastic modulus, $q_{15}$ a piezomagnetic constant, $e_{15}$ a piezoelectric constant, $\varepsilon_{11}$ a dielectric constant and $d_{11}$ a magnetoelectric constant. According to Zheng et al. (2007), the shear stress components $\tau_{31}$ and $\tau_{32}$, shear strain components $\gamma_{31}$ and $\gamma_{32}$, electric displacement components $D_1$ and $D_2$, electrical field components $E_1$ and $E_2$, magnetic induction components $B_1$ and $B_2$, and magnetic field components $H_1$ and $H_2$ can be expressed in terms of an analytical complex function vector $\mathbf{f}(z)$ as

$$\begin{Bmatrix} w \\ \varphi \\ \phi \end{Bmatrix} = \mathrm{Re}\begin{Bmatrix} f_w(z) \\ f_\varphi(z) \\ f_\phi(z) \end{Bmatrix} = \mathrm{Re}\big[\mathbf{f}(z)\big], \tag{4}$$

$$\begin{Bmatrix} \tau_{31} - \mathrm{i}\tau_{32} \\ D_1 - \mathrm{i}D_2 \\ B_1 - \mathrm{i}B_2 \end{Bmatrix} = \begin{bmatrix} c_{44} & e_{15} & q_{15} \\ e_{15} & -\varepsilon_{11} & -d_{11} \\ q_{15} & -d_{11} & -\mu_{11} \end{bmatrix} \mathbf{f}'(z) = \mathbf{C}\mathbf{f}'(z), \tag{5}$$

$$\begin{Bmatrix} \gamma_{31} - \mathrm{i}\gamma_{32} \\ -E_1 + \mathrm{i}E_2 \\ -H_1 + \mathrm{i}H_2 \end{Bmatrix} = \mathbf{f}'(z), \tag{6}$$

where Re denotes the real part and prime indicates differentiation with respect to the complex variable $z = x_1 + \mathrm{i}x_2$.

In order to express the boundary condition in terms of $\mathbf{f}(z)$ rather than its derivative $\mathbf{f}'(z)$, we integrate the traction $t$, the normal electric displacement $D_n$ and the normal magnetic induction $B_n$ as

$$\int \begin{Bmatrix} t \\ D_n \\ B_n \end{Bmatrix} ds = \mathrm{Im}\big[\mathbf{C}\mathbf{f}(z)\big], \tag{7}$$

where Im denotes the imaginary part of a complex function.

## 3. Solution of a homogeneous medium problem

Now we examine the homogeneous medium solution $\mathbf{f}_0(z)$ of a generalized screw dislocation in a homogeneous medium which is subjected to remote magnetoelectromechanical loadings. Let the generalized screw dislocation with vector $\mathbf{b} = [b_z, b_\varphi, b_\phi]^t$ and generalized line force $\mathbf{p} = [-p_z, p_\varphi, p_\phi]^t$ be applied at a point $z_0$, where $b_z, b_\varphi, b_\phi$ represent the jump in displacement, electrical potential and magnetic potential across the slip plane respectively, and $p_z, p_\varphi, p_\phi$, represent a line force, a line electric charge and a line magnetic charge respectively. Referring to the work of Zheng et al. (2007), the complex potential corresponding to this homogeneous medium problem can be expressed as

$$\begin{aligned} \mathbf{f}_0(z) &= \frac{1}{2\pi\mathrm{i}}(\mathbf{b} + \mathrm{i}\mathbf{C}^{-1}\mathbf{p})\log(z - z_0) + \mathbf{C}^{-1}\boldsymbol{\Gamma}z \\ &= \mathbf{D}\log(z - z_0) + \mathbf{C}^{-1}\boldsymbol{\Gamma}z, \end{aligned} \tag{8}$$

where $\boldsymbol{\Gamma} = [\tau_{31}^\infty - \mathrm{i}\tau_{32}^\infty, D_1^\infty - \mathrm{i}D_2^\infty, B_1^\infty - \mathrm{i}B_2^\infty]^t$ represents the remote magnetoelectromechanical loading.

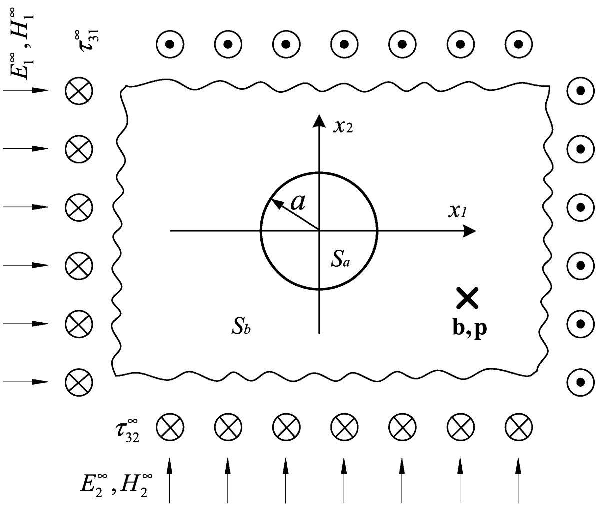


Fig. 2. A circular inclusion under magnetoelectromechanical loading.

## 4. A circular inclusion in a magnetoelectroelastic solid

Consider a two-phase magnetoelectroelastic composite bonded along the circular interface $r = a$ with a magneto-electric loading applied in the matrix (Fig. 2). Our objective is to construct a bi-material solution in the form

$$\mathbf{f}(z) = \begin{cases} \mathbf{f}_a(z), & z \in S_a, \\ \mathbf{f}_b(z) + \mathbf{f}_0(z), & z \in S_b, \end{cases} \tag{9}$$

where $S_a$, the inner region, and $S_b$, the outer region, are occupied by material $a$ and $b$ respectively, and $\mathbf{f}_0(z)$ represents the solution corresponding to the homogeneous medium which is holomorphic in the entire domain except for some singular points. In order to express $\mathbf{f}_a(z)$ and $\mathbf{f}_b(z)$(holomorphic in $S_a$ and $S_b$, respectively) in terms of $\mathbf{f}_0(z)$, continuity of displacement, electric potential and magnetic potential across the interface, by the analytical continuation theorem, is used to yield the requirement

$$\begin{cases} \mathbf{f}_a(z) - \overline{\mathbf{f}_b}\left(\dfrac{a^2}{z}\right) - \mathbf{f}_0(z) = 0, & z \in S_a, \\ \overline{\mathbf{f}_a}\left(\dfrac{a^2}{z}\right) - \mathbf{f}_b(z) - \overline{\mathbf{f}_0}\left(\dfrac{a^2}{z}\right) = 0, & z \in S_b. \end{cases} \tag{10}$$

Continuity of traction and normal component of the electric displacement and magnetic induction, by the same arguments, results in

$$\begin{cases} \mathbf{C}_a\mathbf{f}_a(z) + \mathbf{C}_b\overline{\mathbf{f}_b}\left(\dfrac{a^2}{z}\right) - \mathbf{C}_b\mathbf{f}_0(z) = 0, & z \in S_a, \\ \mathbf{C}_a\overline{\mathbf{f}_a}\left(\dfrac{a^2}{z}\right) + \mathbf{C}_b\mathbf{f}_b(z) - \mathbf{C}_b\overline{\mathbf{f}_0}\left(\dfrac{a^2}{z}\right) = 0, & z \in S_b, \end{cases} \tag{11}$$

where

$$\mathbf{C}_a = \begin{bmatrix} c_{44}^{(a)} & e_{15}^{(a)} & q_{15}^{(a)} \\ e_{15}^{(a)} & -\varepsilon_{11}^{(a)} & -d_{11}^{(a)} \\ q_{15}^{(a)} & -d_{11}^{(a)} & -\mu_{11}^{(a)} \end{bmatrix},$$

$$\mathbf{C}_b = \begin{bmatrix} c_{44}^{(b)} & e_{15}^{(b)} & q_{15}^{(b)} \\ e_{15}^{(b)} & -\varepsilon_{11}^{(b)} & -d_{11}^{(b)} \\ q_{15}^{(b)} & -d_{11}^{(b)} & -\mu_{11}^{(b)} \end{bmatrix}.$$

From Eqs. (10) and (11), we have

$$\begin{cases} \mathbf{f}_a(z) = \boldsymbol{\alpha}_{ab}\mathbf{f}_0(z), \\ \mathbf{f}_b(z) = \boldsymbol{\beta}_{ab}\overline{\mathbf{f}_0}\left(\dfrac{a^2}{z}\right), \end{cases} \tag{12}$$

where

$$\boldsymbol{\alpha}_{ab} = 2(\mathbf{C}_a + \mathbf{C}_b)^{-1}\mathbf{C}_b, \tag{13}$$

$$\boldsymbol{\beta}_{ab} = (\mathbf{C}_a + \mathbf{C}_b)^{-1}(\mathbf{C}_b - \mathbf{C}_a). \tag{14}$$

For a magnetoelectric loading applied to the inner region, since the homogeneous medium solution is holomorphic in neither the region $S_a$ nor the region $S_b$, it should be rewritten as

$$\mathbf{f}_0(z) = \mathbf{D}_a \log z + \mathbf{f}_0^*(z),$$

where $\mathbf{D}_a$ is defined as in Eq. (8), but the magnetoelectroelastic constants involved in $\mathbf{D}_a$ are for material $a$, and

$$\mathbf{f}_0^*(z) = \mathbf{D}_a \log\left(1 - \frac{z_0}{z}\right),$$

which is holomorphic in the outer region $S_b$. By applying the continuity conditions of $\mathrm{Re}[\mathbf{f}(z)]$ and $\mathrm{Im}[\mathbf{C}\mathbf{f}(z)]$ along the interface, and using the method of analytic continuation, one can obtain

$$\mathbf{f}(z) = \begin{cases} \mathbf{f}_0(z) + \mathbf{f}_a(z), & z \in S_a, \\ \mathbf{D}_b \log\left(\dfrac{z}{a}\right) + \mathbf{D}_a \log(a) + \mathbf{f}_b(z), & z \in S_b, \end{cases} \tag{15}$$

where

$$\begin{cases} \mathbf{f}_a(z) = \boldsymbol{\beta}_{ba}\overline{\mathbf{f}_0^*}\left(\dfrac{a^2}{z}\right), \\ \mathbf{f}_b(z) = \boldsymbol{\alpha}_{ba}\mathbf{f}_0^*(z), \end{cases} \tag{16}$$

and $\mathbf{D}_b$ is defined as in Eq. (8), but the magnetoelectroelastic constants involved in $\mathbf{D}_b$ are for material $b$.

## 5. A circular layered inclusion in a magnetoelectroelastic solid

In this section, we consider a three-phase magnetoelectroelastic composite (Fig. 1), whose cross-section consists of a circular ring $S_b$, with outer and inner radii designated by $b$ and $a$, respectively. Its inner and outer boundaries are perfectly bonded to a circular inclusion $S_a$ and a matrix $S_c$, respectively.

### *5.1. Case I: A generalized screw dislocation located in the interphase layer $S_b$*

A series solution for the present three-phase magnetoelectroelastic composite with a generalized screw dislocation located in the interphase layer $S_b$ is assumed, in the form

$$\mathbf{f}(z) = \begin{cases} \displaystyle\sum_{n=1}^{\infty} \mathbf{f}_{an}(z), & z \in S_a, \\ \mathbf{f}_0(z) + \displaystyle\sum_{n=1}^{\infty} \mathbf{f}_n(z) + \sum_{n=1}^{\infty} \mathbf{f}_{bn}(z), & z \in S_b, \\ \mathbf{D}_c \log\left(\dfrac{z}{b}\right) + \mathbf{D}_b \log(b) + \mathbf{f}_{c0}(z) + \displaystyle\sum_{n=1}^{\infty} \mathbf{f}_{cn}(z), & z \in S_c, \end{cases} \tag{17}$$

where $\mathbf{D}_c$ is defined as $\mathbf{D}_a$ in Section 4, but the magnetoelectroelastic constants involved in $\mathbf{D}_c$ are for material $c$. Now, it is required to solve for $\mathbf{f}_{c0}(z), \mathbf{f}_{an}(z), \mathbf{f}_{bn}(z), \mathbf{f}_{cn}(z)$ and $\mathbf{f}_n(z)$ $(n = 1, 2, 3, \ldots)$, analytic in their respective regions, in terms of $\mathbf{f}_0(z)$, by the procedure as follows.

Step 1. Analytic continuation across the interface $L$.

First, we regard regions $S_a$ and $S_b$ as being composed of the same material $b$, and region $S_c$ of material $c$. Since $\mathbf{f}_0(z)$ is a homogeneous medium solution and $\mathbf{f}_{c0}(z)$ and $\mathbf{f}_1(z)$ are introduced to satisfy the continuity conditions across the interface $L$, Eqs. (15) and (16) lead to

$$\begin{cases} \mathbf{f}_1(z) = \boldsymbol{\beta}_{cb}\overline{\mathbf{f}_0^*}\left(\dfrac{b^2}{z}\right), & z \in S_a \cup S_b, \\ \mathbf{f}_{c0}(z) = \boldsymbol{\alpha}_{cb}\mathbf{f}_0^*(z), & z \in S_c, \end{cases} \tag{18}$$

where $\mathbf{f}_0^*(z) = \mathbf{D}_b \log(1 - z_0/z)$. Since we assume that region $S_a$ is made up of material $b$, the fields produced by $\mathbf{f}_1(z)$ cannot satisfy the continuity conditions at the interface $L^*$, which lies between material $a$ and $b$.

Step 2. Analytic continuation across the interface $L^*$.

Next, we assume that region $S_a$ is composed of material $a$ and regions $S_b$ and $S_c$ are regarded as made up of the same material $b$. $\mathbf{f}_1(z)$ in Eq. (18) having the singular points in $S_b \cup S_c$ is treated as a homogeneous solution of material $b$. As in Eqs. (9) and (12), $\mathbf{f}_{a1}(z)$ and $\mathbf{f}_{b1}(z)$ are introduced to satisfy the continuity conditions across the interface $L^*$ as

$$\begin{cases} \mathbf{f}_{a1}(z) = \boldsymbol{\alpha}_{ab}\big[\mathbf{f}_1(z) + \mathbf{f}_0(z)\big], & z \in S_a, \\ \mathbf{f}_{b1}(z) = \boldsymbol{\beta}_{ab}\left[\overline{\mathbf{f}_1}\left(\dfrac{a^2}{z}\right) + \overline{\mathbf{f}_0}\left(\dfrac{a^2}{z}\right)\right], & z \in S_b \cup S_c. \end{cases} \tag{19}$$

Since this result is based on the assumption that region $S_c$ is made up of material $b$, the field produced by $\mathbf{f}_{b1}(z)$ cannot satisfy the continuity conditions at the interface $L$.

Step 3. Analytic continuation across the interface $L$.

We again assume regions $S_a$ and $S_b$ be made up of the same material $b$ and region $S_c$ of material $c$. As in Eqs. (15) and (16), $\mathbf{f}_{b1}(z)$ is taken to be a homogeneous solution of material $b$, and $\mathbf{f}_2(z)$ and $\mathbf{f}_{c1}(z)$ are introduced to satisfy the continuity conditions across the interface $L$. Accordingly, it can be shown

$$\begin{cases} \mathbf{f}_2(z) = \boldsymbol{\beta}_{cb}\overline{\mathbf{f}_{b1}}\left(\dfrac{b^2}{z}\right), & z \in S_a \cup S_b, \\ \mathbf{f}_{c1}(z) = \boldsymbol{\alpha}_{cb}\mathbf{f}_{b1}(z), & z \in S_c. \end{cases} \tag{20}$$

Similarly, the fields produced by $\mathbf{f}_2(z)$ do not satisfy the conditions at the interface $L^*$.

Step 4. Repetitions of steps 2 and 3.

By repeating steps 2 and 3 for $n = 2, 3, 4, \ldots$, one can express all the functions $\mathbf{f}_{c0}(z), \mathbf{f}_{an}(z), \mathbf{f}_{bn}(z)$, and $\mathbf{f}_{cn}(z)$ $(n = 1, 2, 3, \ldots)$ in terms of $\mathbf{f}_0(z)$ as

$$\mathbf{f}(z) = \begin{cases} \boldsymbol{\alpha}_{ab}\displaystyle\sum_{n=0}^{\infty}(\boldsymbol{\beta}_{cb}\boldsymbol{\beta}_{ab})^n\left[\mathbf{f}_0\left(\frac{a^{2n}}{b^{2n}}z\right) + \boldsymbol{\beta}_{cb}\overline{\mathbf{f}_0^*}\left(\frac{b^{2n+2}}{a^{2n}}\frac{1}{z}\right)\right], & z \in S_a, \\ \displaystyle\sum_{n=0}^{\infty}(\boldsymbol{\beta}_{cb}\boldsymbol{\beta}_{ab})^n\left[\mathbf{f}_0\left(\frac{a^{2n}}{b^{2n}}z\right) + \boldsymbol{\beta}_{cb}\overline{\mathbf{f}_0^*}\left(\frac{b^{2n+2}}{a^{2n}}\frac{1}{z}\right)\right] & \\ \quad + \boldsymbol{\beta}_{ab}\displaystyle\sum_{n=0}^{\infty}(\boldsymbol{\beta}_{cb}\boldsymbol{\beta}_{ab})^n\left[\overline{\mathbf{f}_0}\left(\frac{a^{2n+2}}{b^{2n}}\frac{1}{z}\right) + \boldsymbol{\beta}_{cb}\mathbf{f}_0^*\left(\frac{b^{2n+2}}{a^{2n+2}}z\right)\right], & z \in S_b, \\ \mathbf{D}_c\log\left(\dfrac{z}{b}\right) + \mathbf{D}_b\log(b) + \boldsymbol{\alpha}_{cb}\mathbf{f}_0^*(z) & \\ \quad + \boldsymbol{\alpha}_{cb}\boldsymbol{\beta}_{ab}\displaystyle\sum_{n=0}^{\infty}(\boldsymbol{\beta}_{cb}\boldsymbol{\beta}_{ab})^n\left[\overline{\mathbf{f}_0}\left(\frac{a^{2n+2}}{b^{2n}}\frac{1}{z}\right) + \boldsymbol{\beta}_{cb}\mathbf{f}_0^*\left(\frac{b^{2n+2}}{a^{2n+2}}z\right)\right], & z \in S_c. \end{cases} \tag{21}$$

### 5.2. Case II: A generalized screw dislocation located in the matrix $S_c$

Using the same procedure as case I, the case in which the generalized screw dislocation located in the matrix $S_c$ has the following solution

$$\mathbf{f}(z)=\begin{cases}\boldsymbol{\alpha}_{ab}\sum_{n=0}^{\infty}(\boldsymbol{\beta}_{cb}\boldsymbol{\beta}_{ab})^n\boldsymbol{\alpha}_{bc}\mathbf{f}_0\left(\frac{a^{2n}}{b^{2n}}z\right), & z\in S_a,\\ \sum_{n=0}^{\infty}(\boldsymbol{\beta}_{cb}\boldsymbol{\beta}_{ab})^n\boldsymbol{\alpha}_{bc}\mathbf{f}_0\left(\frac{a^{2n}}{b^{2n}}z\right)+\boldsymbol{\beta}_{ab}\sum_{n=0}^{\infty}(\boldsymbol{\beta}_{cb}\boldsymbol{\beta}_{ab})^n\boldsymbol{\alpha}_{bc}\overline{\mathbf{f}}_0\left(\frac{a^{2n+2}}{b^{2n}}\frac{1}{z}\right), & z\in S_b,\\ \mathbf{f}_0(z)+\boldsymbol{\beta}_{bc}\overline{\mathbf{f}}_0\left(\frac{b^2}{z}\right)+\boldsymbol{\alpha}_{cb}\boldsymbol{\beta}_{ab}\sum_{n=0}^{\infty}(\boldsymbol{\beta}_{cb}\boldsymbol{\beta}_{ab})^n\boldsymbol{\alpha}_{bc}\overline{\mathbf{f}}_0\left(\frac{a^{2n+2}}{b^{2n}}\frac{1}{z}\right), & z\in S_c.\end{cases}\tag{22}$$

### 5.3. Case III: A generalized screw dislocation located in the inner inclusion $S_a$

Similarly, the solution for the case in which the generalized screw dislocation located in the inner inclusion $S_a$ can be derived as

$$\mathbf{f}(z)=\begin{cases}\mathbf{f}_0(z)+\boldsymbol{\beta}_{ba}\overline{\mathbf{f}}_0^*\left(\frac{a^2}{z}\right)+\boldsymbol{\alpha}_{ab}\boldsymbol{\beta}_{cb}\sum_{n=0}^{\infty}(\boldsymbol{\beta}_{ab}\boldsymbol{\beta}_{cb})^n\boldsymbol{\alpha}_{bc}\overline{\mathbf{f}}_0^*\left(\frac{b^{2n+2}}{a^{2n}}\frac{1}{z}\right), & z\in S_a,\\ \mathbf{D}_b\log\left(\frac{z}{a}\right)+\mathbf{D}_a\log a+\sum_{n=0}^{\infty}(\boldsymbol{\beta}_{ab}\boldsymbol{\beta}_{cb})^n\boldsymbol{\alpha}_{ba}\mathbf{f}_0^*\left(\frac{b^{2n}}{a^{2n}}z\right) & \\ \quad+\boldsymbol{\beta}_{cb}\sum_{n=0}^{\infty}(\boldsymbol{\beta}_{ab}\boldsymbol{\beta}_{cb})^n\boldsymbol{\alpha}_{bc}\overline{\mathbf{f}}_0^*\left(\frac{b^{2n+2}}{a^{2n}}\frac{1}{z}\right), & z\in S_b,\\ \mathbf{D}_c\log\left(\frac{z}{b}\right)+\mathbf{D}_b\log\left(\frac{b}{a}\right)+\mathbf{D}_a\log a+\boldsymbol{\alpha}_{cb}\sum_{n=0}^{\infty}(\boldsymbol{\beta}_{ab}\boldsymbol{\beta}_{cb})^n\boldsymbol{\alpha}_{ba}\mathbf{f}_0^*\left(\frac{b^{2n}}{a^{2n}}z\right), & z\in S_c.\end{cases}\tag{23}$$

Eqs. (21), (22) and (23) give a general series solution of the problem associated with the three-phase circular layered composite under arbitrary loading as the corresponding homogeneous medium solution $\mathbf{f}_0(z)$ is solved. Applying the derived analytical solutions and assuming the dislocation density along the crack as an unknown function, one can obtain the standard singular integral equations for the corresponding magnetoelectric crack problem. A numerical solution of the dislocation density function can be obtained by solving the resulting linear algebraic equations. Similar numerical processes can be found in the literature, e.g. Chen and Hesebe (1992), Chao and Shen (1995) and Wang and Zhong (2003).

## 6. Results and discussion

In this section, the fundamental series solution derived in the preceding section will be used to analyze the following examples associated with a circular layered piezoelectric/piezomagnetic composite subjected to magnetoelectromechanical loading. Numerical results are obtained for the composite $BaTiO_3$–$CoFe_2O_4$, the constituents of which are: piezoelectric $BaTiO_3$ and piezomagnetic $CoFe_2O_4$, whose material constants are given as Zheng et al. (2007)

- piezoelectric $BaTiO_3$:
  $c_{44}=43\times10^9\ \mathrm{N/m^2}$, $e_{15}=11.6\ \mathrm{C/m^2}$, $q_{15}=0$, $\varepsilon_{11}=11.2\times10^{-9}\ \mathrm{C^2/\,N\,m^2}$, $d_{11}=0$, $\mu_{11}=5.0\times10^{-6}\ \mathrm{N\,s^2/C^2}$.
- piezomagnetic $CoFe_2O_4$:
  $c_{44}=45.3\times10^9\ \mathrm{N/m^2}$, $e_{15}=0$, $q_{15}=550\ \mathrm{N/A\,m}$, $\varepsilon_{11}=0.08\times10^{-9}\ \mathrm{C^2/N\,m^2}$, $d_{11}=0$, $\mu_{11}=-590\times10^{-6}\ \mathrm{N\,s^2/C^2}$.

*6.1. Uniform far-field magnetoelectroelastic loading*

We first consider the problem of a tri-magnetoelectric composite subjected to a uniform far-field anti-plane shear $\tau_{31}^{\infty}$. Figs. 3–5 show the variations of the shear stress $\tau_{31}$, electric displacement $D_1$ and magnetic induction

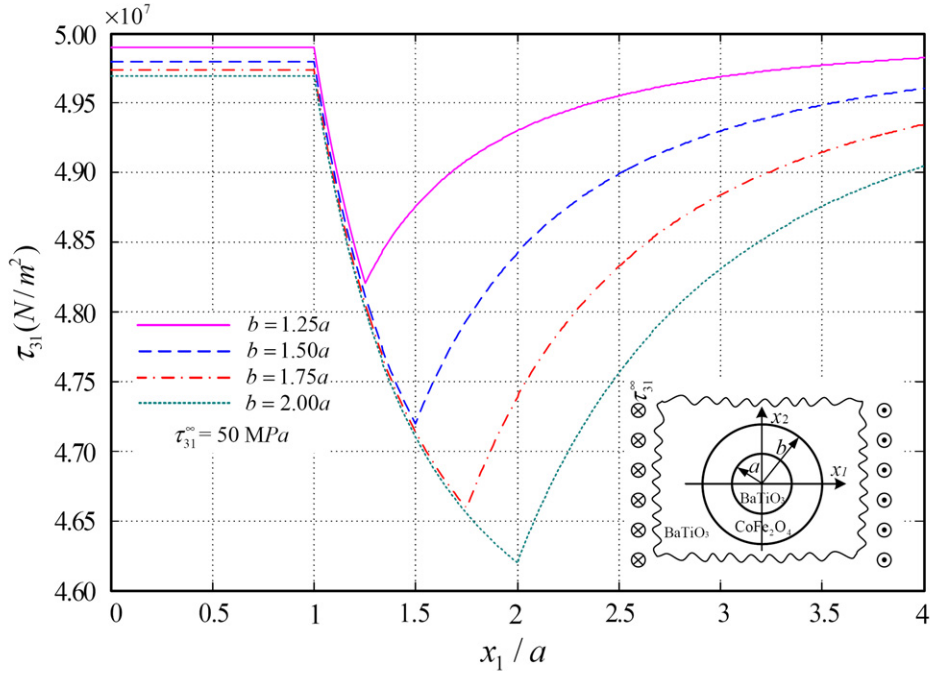


Fig. 3. The variation of the shear stress $\tau_{31}$ along the real axis $x_1$.

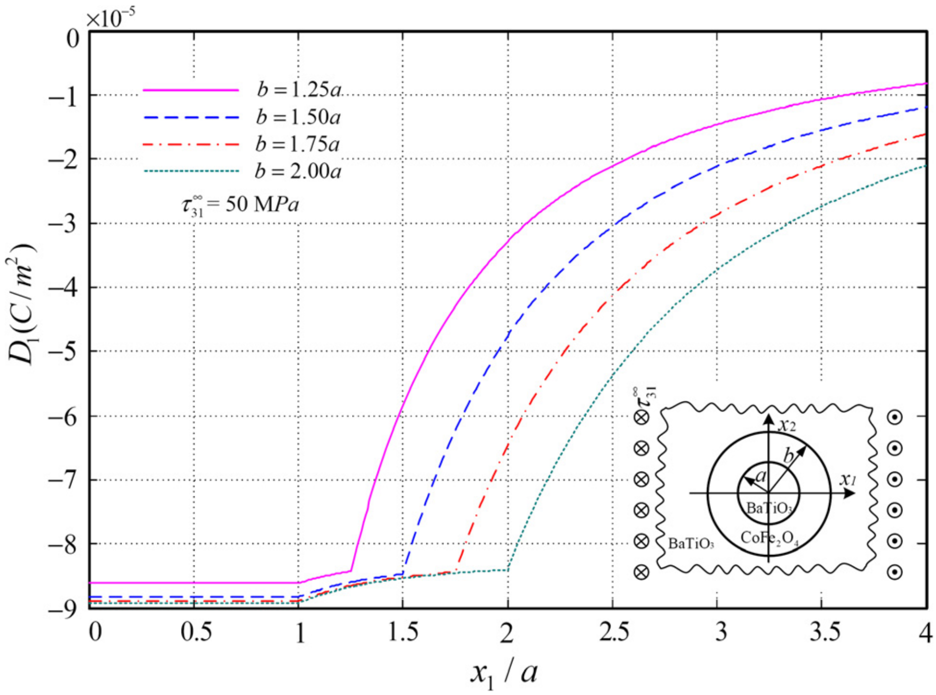


Fig. 4. The variation of the electric displacement $D_1$ along the real axis $x_1$.

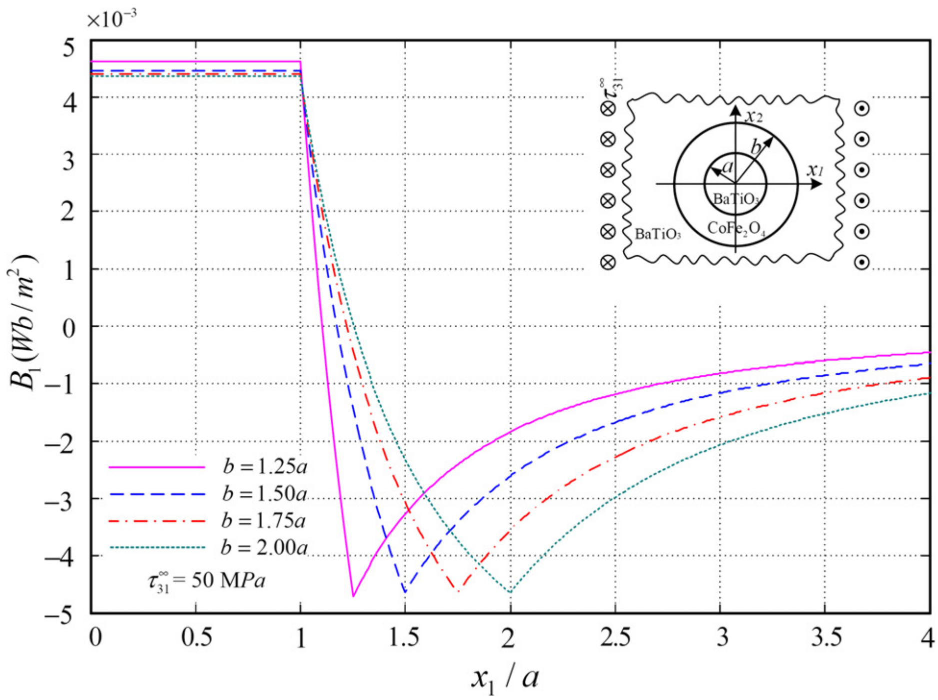


Fig. 5. The variation of the magnetic induction $B_1$ along the real axis $x_1$.

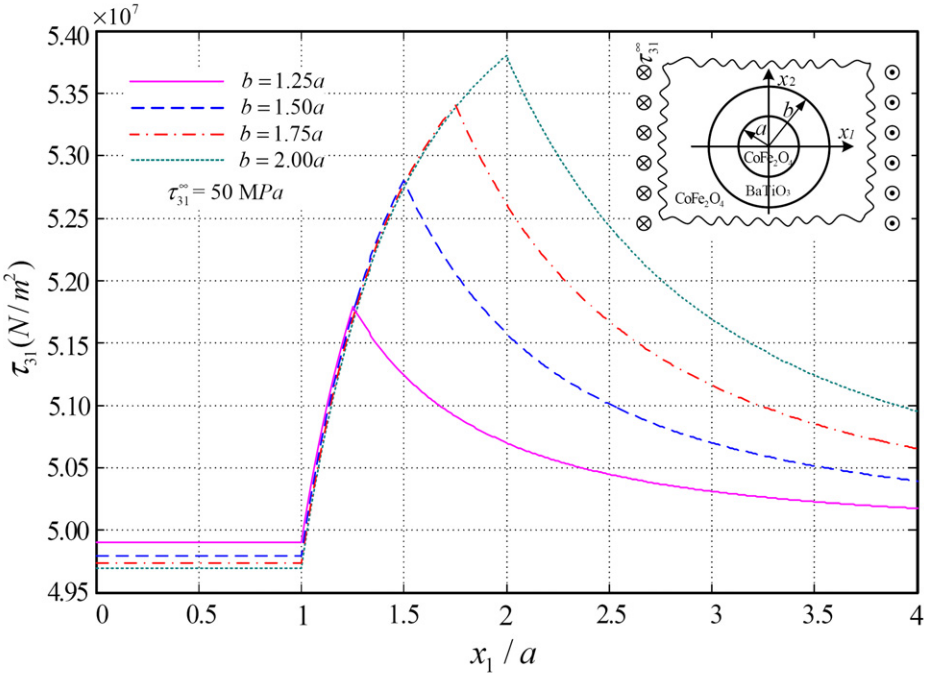


Fig. 6. The variation of the shear stress $\tau_{31}$ along the real axis $x_1$.

$B_1$ along the real axis $x_1$ for the case when the inner inclusion and the matrix are piezoelectric $BaTiO_3$ and the interphase layer is piezomagnetic $CoFe_2O_4$. Figs. 6–8 show the variations of the shear $\tau_{31}$, electric displacement $D_1$ and magnetic induction $B_1$ along the real axis $x_1$ for the case when the inner inclusion and the matrix are piezomagnetic $CoFe_2O_4$ and the interphase layer is piezoelectric $BaTiO_3$. From these figures, we make the following deductions:

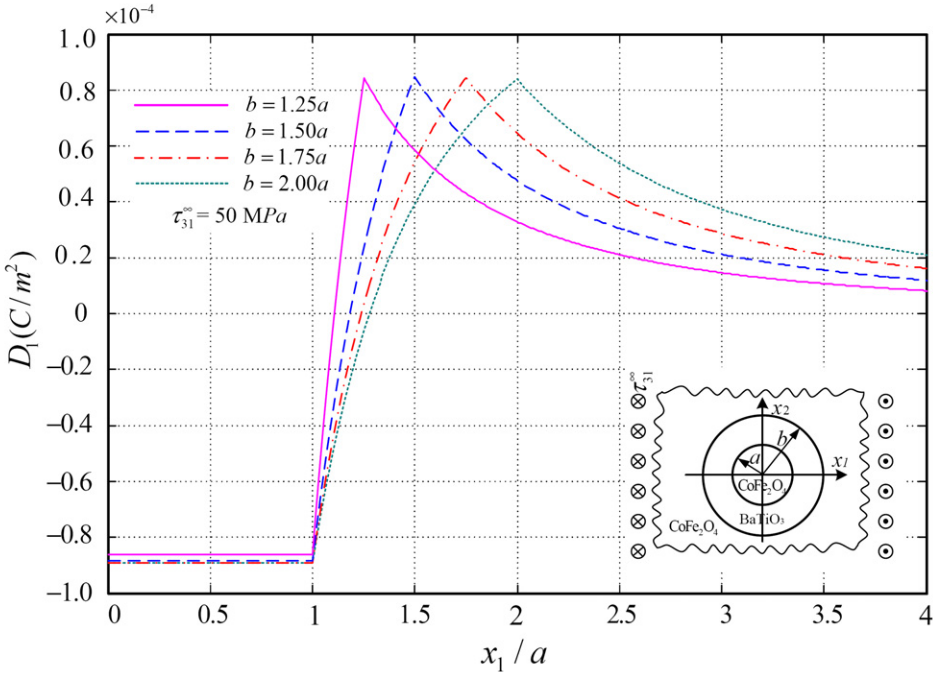


Fig. 7. The variation of the electric displacement $D_1$ along the real axis $x_1$.

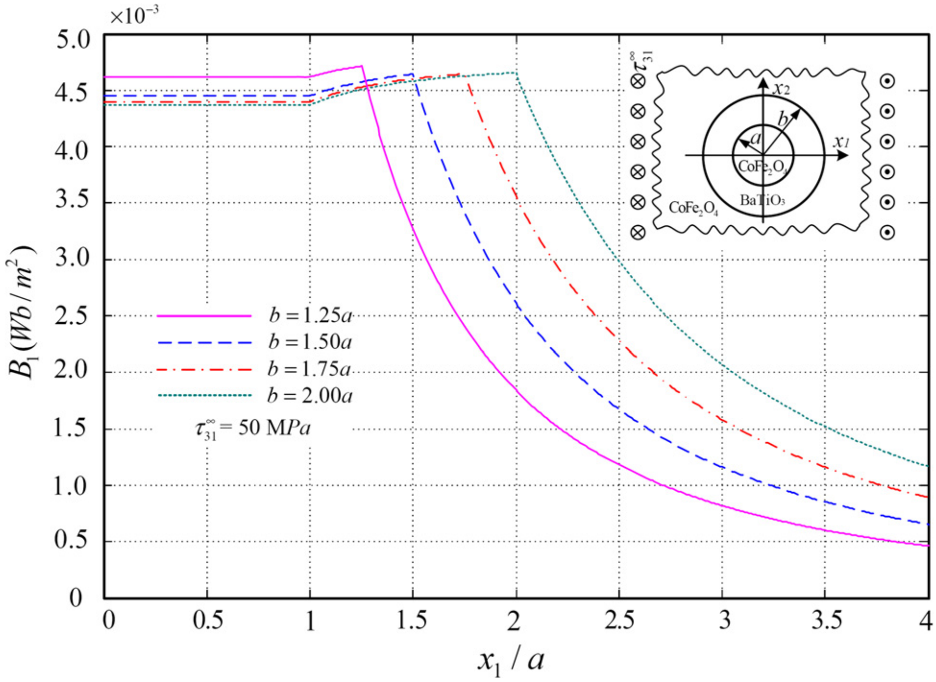


Fig. 8. The variation of the magnetic induction $B_1$ along the real axis $x_1$.

1. The piezoelectric/piezomagnetic composite subjected to a far-field mechanical loading $\tau_{31}^{\infty}$ will exhibit the magnetoelectroelastic coupling effect.
2. The shear stress $\tau_{31}$, electric displacement $D_1$ and magnetic induction $B_1$ produced in the inner inclusion are uniform.

3. The shear stress $\tau_{31}$, electric displacement $D_1$ and magnetic induction $B_1$ are continuous across the interface, which conforms to the boundary conditions.
4. When the interphase layer is piezomagnetic $CoFe_2O_4$, the variation of magnetic induction $B_1$ in the interphase layer is higher than when the interphase layer is piezoelectric $BaTiO_3$. Similarly, when the interphase layer is piezoelectric $BaTiO_3$, the variation of electric displacement $D_1$ in the interphase layer is higher than those when the interphase layer is piezomagnetic $CoFe_2O_4$.
5. For large $x_1$, the shear stress $\tau_{31}$, electric displacement $D_1$ and magnetic induction $B_1$ will tend to the applied loading. Further, $\tau_{31} = \tau_{31}^{\infty}$, $D_1 = 0$ and $B_1 = 0$, which also conforms to the boundary conditions.

### 6.2. Image force on the generalized screw dislocation

The image force acting on the dislocation is an important physical quantity for understanding the interaction of a dislocation with inhomogeneities. The image force can be calculated by means of the generalized Peach–Koehler formula, by Pak (1990).

$$\begin{aligned} F_1 &= b_z\tau_{32}^T + b_\varphi D_2^T + b_\phi B_2^T, \\ F_2 &= -b_z\tau_{31}^T - b_\varphi D_1^T - b_\phi B_1^T, \end{aligned} \tag{24}$$

where $\tau_{31}^T$, $\tau_{32}^T$, $D_1^T$, $D_2^T$, $B_1^T$ and $B_2^T$ are the perturbation shear stress, electric displacement and magnetic induction components at the dislocation. Suppose a generalized screw dislocation with Burgers vector $b_z$ or electric potential jump $b_\varphi$ is located at the point $z_0$ along the real axis in the matrix or in the circular layered inclusion. Define the normalized force on the dislocation as $F_{10}(b_z) = 2\pi aF_1/c_{44}b_z^2$, $F_{20}(b_z) = 2\pi aF_2/c_{44}b_z^2$, $F_{10}(b_\varphi) = 2\pi aF_1/\varepsilon_{11}b_\varphi^2$, $F_{20}(b_\varphi) = 2\pi aF_2/\varepsilon_{11}b_\varphi^2$. Figs. 9 and 10 respectively show the variation of normalized image force $F_{10}(b_z)$ with location of the dislocation, for the case (a) when the inner inclusion and the matrix are piezoelectric ($BaTiO_3$) and the interphase layer is piezomagnetic ($CoFe_2O_4$) and (b) when the inner inclusion and the matrix are piezomagnetic ($CoFe_2O_4$) and the interphase layer is piezoelectric ($BaTiO_3$). It is seen that the interfaces will repel the dislocation having Burgers vector, $b_z$, located in any region. The origin, a point near the middle of the interphase layer and the point at infinity are three stable equilibrium positions in which the image forces are equal to zero. Figs. 11

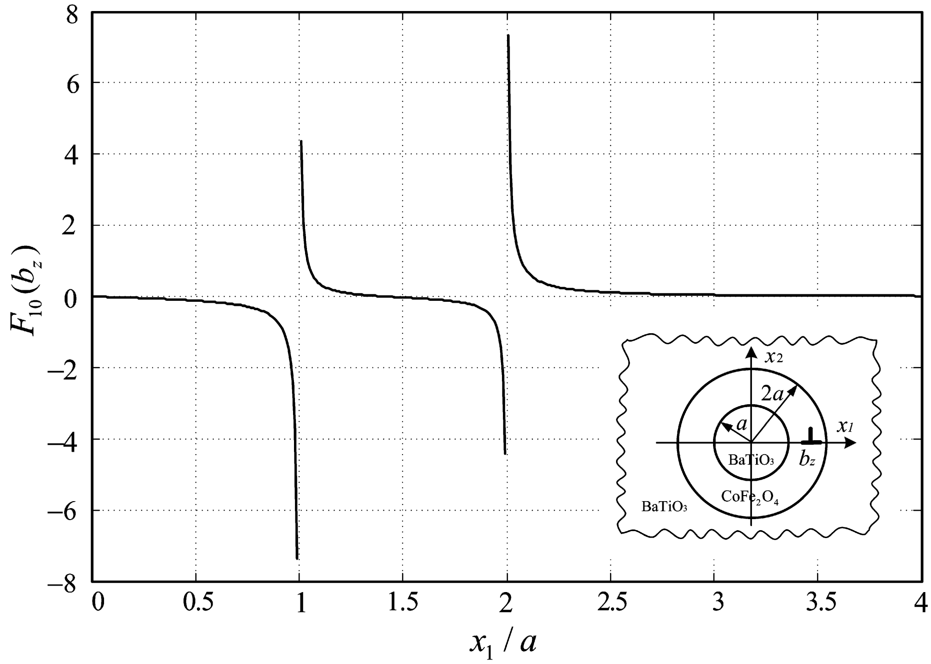


Fig. 9. The variation of normalized image force $F_{10}(b_z)$ with location of the dislocation.

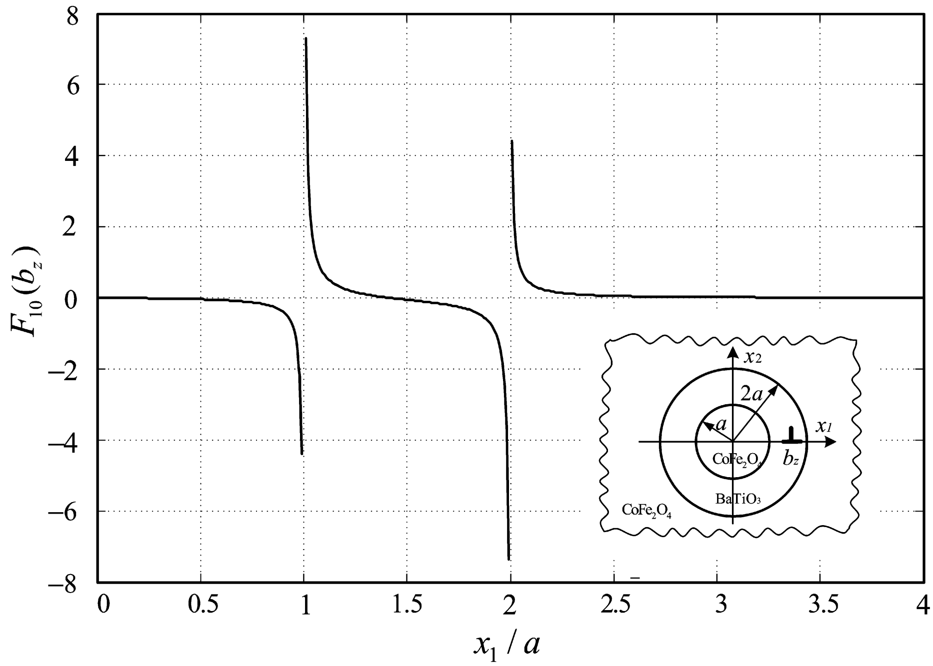


Fig. 10. The variation of normalized image force $F_{10}(b_z)$ with location of the dislocation.

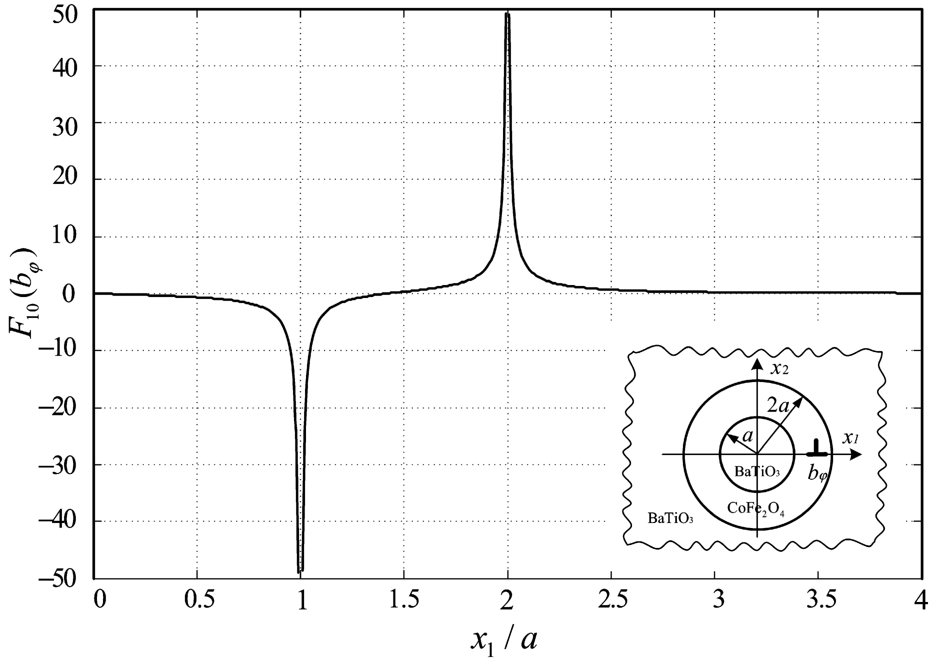


Fig. 11. The variation of normalized image force $F_{10}(b_\varphi)$ with location of the dislocation.

and 12 show the variations of normalized image force $F_{10}(b_\varphi)$ with respect to the location of the dislocation. It is seen that the interfaces will attract the dislocation having Burgers vector, $b_\varphi$, located in the interphase layer. A point near the middle of the interphase layer is an unstable equilibrium position when the interphase layer is piezomagnetic

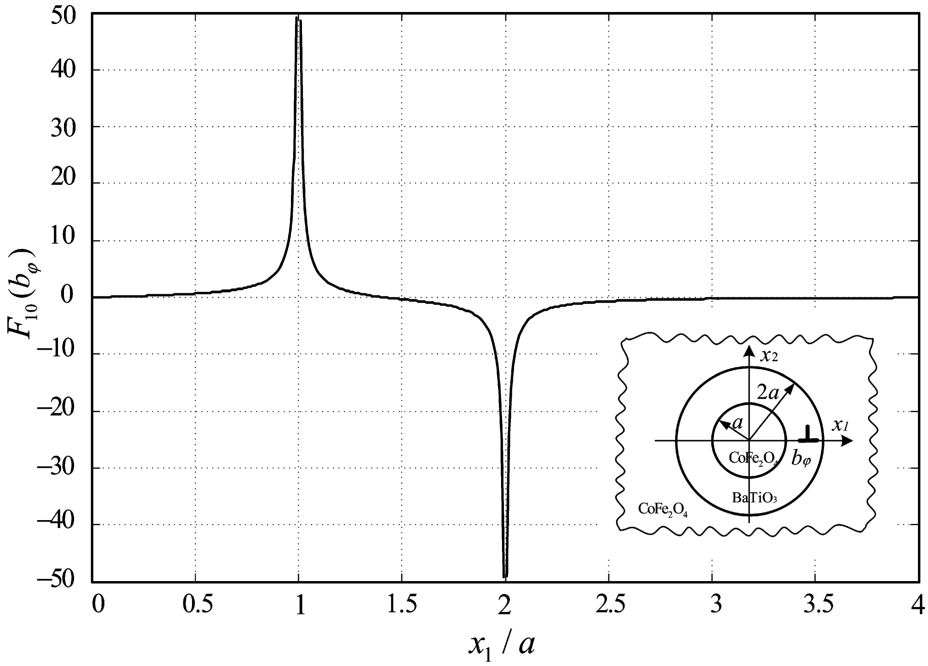


Fig. 12. The variation of normalized image force $F_{10}(b_\varphi)$ with location of the dislocation.

$CoFe_2O_4$, while the interfaces will repel the dislocation, $b_\varphi$, located in the interphase layer. A point near the middle of the interphase layer is a stable equilibrium position when the interphase layer is piezoelectric $BaTiO_3$.

## 7. Concluding remarks

In this paper, the problem of a circular layered composite under magnetoelectromechanical loading is solved. Based on the method of analytic continuation and the alternating technique, the solution is obtained as a transformation of the solution to the corresponding homogeneous medium solution. Numerical results show that for the special case of uniform remote loading, the shear stress, electric displacement and magnetic induction produced in the inner inclusion are uniform. When the interphase layer is piezomagnetic $CoFe_2O_4$ the variations of magnetic induction $B_1$ in the interphase layer are higher than those when the interphase layer is piezoelectric $BaTiO_3$. Similarly, when the interphase layer is piezoelectric $BaTiO_3$ the variations of electric displacement $D_1$ in the interphase layer are higher than those when the interphase layer is piezomagnetic $CoFe_2O_4$. These important phenomena show the feasibility of building a very sensitive sensor in magnetoelectric composites.

## Acknowledgements

This work was supported by the National Science Council of ROC under the contract number NSC 95-2221-E-252-005.

## References

Chao, C.K., Shen, M.H., 1995. Solutions of thermoelastic crack problems in bonded dissimilar media or half-plane medium. International Journal of Solids and Structures 32, 3537–3554.

Chen, Y.Z., Hesebe, N., 1992. New integral equation for the thermally insulated curve crack problem in an infinite plane. Journal of Thermal Stresses 15, 519–532.

Chen, Z.R., Yu, S.W., Meng, L., Lin, Y., 2002. Effective properties of layered magneto-electro-elastic composites. Composite Structures 57, 177–182.

Fang, Q.H., Liu, Y.W., Jiang, C.P., 2005. On the interaction between a generalized screw dislocation and circular-arc interfacial rigid lines in magnetoelectroelastic solids. International Journal of Engineering Science 43, 1011–1031.

Hao, R.J., Liu, J.X., 2006. Interaction of a screw dislocation with a semi-infinite interfacial crack in a magneto-electro-elastic bi-material. Mechanics Research Communications 33, 415–424.

Huang, J.H., Kuo, W.S., 1997. The analysis of piezoelectric/piezomagnetic composite materials containing ellipsoidal inclusions. Journal of Applied Physics 81, 1378–1386.

Jiang, C.P., Cheung, Y.K., 2001. An exact solution for the three-phase piezoelectric cylinder model under antiplane shear and its applications to piezoelectric composites. International Journal of Solids and Structures 38, 4777–4796.

Li, J.Y., 2000. Magnetoelectroelastic multi-inclusion and inhomogeneity problems and their applications in composite materials. International Journal of Engineering Science 38, 1993–2011.

Li, J.Y., 2002. Magnetoelectric Green's functions and their application to the inclusion and inhomogeneity problems. International Journal of Solids and Structures 39, 4201–4213.

Li, J.Y., Dunn, M.L., 1998a. Micromechanics of magnetoelectroelastic composite materials: average fields and effective behavior. Journal of Intelligent Material Systems and Structures 7, 404–416.

Li, J.Y., Dunn, M.L., 1998b. Anisotropic coupled field inclusion and inhomogeneity problems. Philosophical Magazine A 77, 1341–1350.

Liu, J.X., Liu, X.L., Zhao, Y.B., 2001. Green's functions for anisotropic magnetoelectroelastic solids with an elliptical cavity or a crack. International Journal of Engineering Science 39, 1405–1418.

Liu, Y.W., Jiang, C.P., Cheung, Y.K., 2003. A screw dislocation interacting with an interphase layer between a circular inhomogeneity and the matrix. International Journal of Engineering Science 41, 1883–1898.

Nan, C.W., 1994. Magnetoelectric effect in composites of piezoelectric and piezomagnetic phases. Physical Review B 50, 6082–6088.

Pak, Y.E., 1990. Force on a piezoelectric screw dislocation. ASME Journal of Applied Mechanics 57, 863–869.

Pan, E., 2001. Exact solution for simply supported and multilayered magneto-electro-elastic plates. ASME Journal of Applied Mechanics 68, 608–618.

Sudak, L.J., 2003. Effect of an interphase layer on the electroelastic stresses within a three-phase elliptic inclusion. International Journal of Engineering Science 41, 1019–1039.

van Run, A.M.J.G., Terrel, D.R., Scholing, J.H., 1974. An in situ grown eutectic magnetoelectric composite material. Journal of Material Science 9, 1710–1714.

van Suchtelen, J., 1972. Product properties: a new application of composite materials. Philips Research Reports 27, 28–37.

Wang, X., Shen, Y.P., 2003. Inclusions of arbitrary shape in magnetoelectroelastic composite materials. International Journal of Engineering Science 41, 85–102.

Wang, X., Zhong, Z., 2003. A circular inclusion with a nonuniform interphase layer in anti-plane shear. International Journal of Solids and Structures 40, 881–897.

Wu, T.L., Huang, J.H., 2000. Closed-form solutions for the magnetoelectric coupling coefficients in fibrous composites with piezoelectric and piezomagnetic phases. International Journal of Solids and Structures 37, 2981–3009.

Xiao, Z.M., Chen, B.Z., 2000. A screw dislocation interacting with a coated fiber. Mechanics of Materials 32, 485–494.

Zheng, J.L., Fang, Q.H., Liu, Y.W., 2007. A generalized screw dislocation interacting with interfacial cracks along a circular inhomogeneity in magnetoelectroelastic solids. Theoretical and Applied Fracture Mechanics 47, 205–218.